Renewable Energy 151 (2020) 355–365

Contents lists available at ScienceDirect

Renewable Energy

journal homepage: www.elsevier.com/locate/renene

Innovative overheating solution for solar thermal collector using a reflective surface included in the air gap

A. Amiche [a, *], S.M.K. El Hassar [b], A. Larabi [c], Z.A. Khan [d], Z. Khan [d, f], F.J. Aguilar [e], P.V. Quiles [e]

[a] University of Sciences & Technology Houari Boumediene (USTHB). Faculty of Civil Engineering. Laboratory of Build Environment (LBE), USTHB, FGC, BP 32 EL ALIA 16111 BAB EZZOUAR ALGIERS, Algeria
[b] USTHB, Faculty of Civil Engineering, Laboratory of Build Environment (LBE), Algeria
[c] USTHB, Faculty of Electronics and Computer Science, Laboratory of Electrics & Industrials Systems (LSEI), Algeria
[d] Bournemouth University, Faculty of Science and Technology, NanoCorr, Energy and Modelling (NCEM) Research Group, Fern Barrow, Talbot Campus, Poole, Dorset, BH12 5BB, UK
[e] University Miguel Hernández, Avda. Universidad S/N, Elche, 03202, Spain
[f] School of Mechanical and Manufacturing Engineering (SMME), National University of Sciences and Technology (NUST), Sector H-12, Islamabad 44000, Pakistan

ARTICLE INFO

Article history:
Received 16 June 2019
Received in revised form
3 November 2019
Accepted 8 November 2019
Available online 11 November 2019

Keywords:
Flat plate solar collector
Overheating problem
Internal shading protection
Experimental tests
Numerical simulations

ABSTRACT

In this work, a new solution to prevent the overheating of solar collectors in the case of stagnation is presented. The solution proposed consists of inserting a reflective sheet inside the solar collector between the absorber and the glass cover to reduce the incoming energy by reflecting solar radiation. This protection is switched ON or OFF according to the absorber temperature. A prototype has been manufactured and tested in outside conditions and in laboratory. The prototype was tested with different percentages of protection. With 50% of protection, the overheating problem is eliminated. A simplified numerical model of the solar collector with the protection was developed and has been validated. The calculated temperature values are very close to the measured data. The experimental and numerical results showed the good behaviour of the proposed solution.

1. Introduction

Natural gas is the main energy source in the building sector in Algeria. The use of solar energy in this country, an abundant renewable energy source, is currently very low. The total installed area of domestic solar water heaters did not exceed 1000 m^2 in 2016 [1]. In order to reduce the fossil fuels consumption, a law promulgated in 1999 focuses mainly on thermal insulation of the building envelope, greater use of efficient equipment and more frequent use of active solar systems. The promotion of the solar systems is now a priority in Algeria, particularly for sanitary hot water production [2].

This work focuses on the study of liquid flat-plate solar collectors with grid style risers in stagnation conditions. Many improvements have been developed since the first solar flat plate collector was produced, predisposing it to overheating problem [3–6].

Overheating occurs during stagnation periods when the fluid flow is interrupted (e.g. power cut, failure of the primary pump) or when the heat demand is low. In these conditions, the absorber temperature increases to a very high level [7]. Without protection against overheating, steam can be produced and the installation components may be damaged. The standard solar fluid is a mix of propylene glycol and water. Overheating causes glycol to degrade and the mix of propylene glycol and water becomes acidic. This process accelerates scaling, causes premature component degradation and copper corrosion [8,9]. To solve the overheating problem, several passive and active approaches exist [10]. The most important of these solutions are reviewed below (non-exhaustive list).

Drain back system is a traditional solution used to prevent overheating and freezing in solar systems. Different mechanisms of

* Corresponding author.
E-mail address: aamiche@usthb.dz (A. Amiche).

https://doi.org/10.1016/j.renene.2019.11.023
0960-1481/

Nomenclature

Capital letters

C	Heat capacity J kg^{-1} K^{-1}
G	Solar radiation W m^{-2}
M	Mass kg
S	Surface area or heat transfer surface area m^2
T	Temperature …. ..K
Ws	Wind speed m s^{-1}

Small letters

e	Thickness m
hc	Convective heat transfer coefficient W m^{-2} K^{-1}
hr	Radiative heat transfer coefficient W m^{-2} K^{-1}
t	Time s

Greek Symbols

α	Absorptance (−)
ε	Emittance (−)
λ	Thermal conductivity W m^{-1} K^{-1}
ρ	Density kg m^{-3}
τ	Transmittance (−)

Indices

abs	Absorber
amb	Ambient air
b	Bottom
c	Glass Cover
f	Transfer fluid
ins	Thermal Insulation
in	Inlet
out	Outlet
mb	Mid bottom
mt	Mid top
p	Protection
s	Sky
t	Top
w	Water

the drain back solution are used [11]. This system requires a drain back tank, space for the pitching of collectors and pipes necessary for solar fluid drainage. Thus, the effects are: high prices and significant maintenance requirements. The overheating is produced in the absorber, but not in the heat transfer fluid.

Also, many systems include static or dynamic dissipators that remove excessive heat. They can be integrated into the rear side of the solar collector, or externally mounted on the primary loop. Dissipators use natural convection or forced convection by adding fans to increase the convection heat transfer with the environment. A novel application called thermoelectric-self-cooling system uses several thermoelectric modules installed in the solar system. These modules transform part of the heat into electricity, which is supplied to the cooling system [12]. Natural dissipators are limited and can't adjust collector temperature in stagnation conditions. Dynamic dissipators can increase complexity and cost of installation.

Natural and forced ventilation of the solar collectors allow protection against overheating by rejecting the excess thermal energy. To protect the collector from overheating, a ventilation channel with a thermally actuated door can be inserted between the absorber plate and the rear insulation [13,14and15]. The actuated door opens at high temperature operations. Ventilation systems cause a permanent decreasing in the solar collector efficiency by introducing atmospheric contaminants and moisture; this can reduce the collector lifetime [9].

The thermotropic layer provides passive overheat protection by switching optical properties of the solar collector (transmittance and reflectance) to reduce the amount of received energy [16]. Thermotropic material can be applied to the glazing and/or to the absorber. New thermotropic thermal solar systems use a mixture of vanadium and aluminium oxides [17,18]. For Algerian climates (Mediterranean and desert), this solution just reduces the temperature of the absorber without eliminating the overheating problem [19].

To minimize the solar radiation incoming into the collector in stagnation, inverse tracking method can be used [20]. This method is an adequate solution for protecting tracked collectors against overheating. Nevertheless, solar collectors with a tracking system are more expensive than traditional fixed collectors and require more maintenance.

Another solution is the use of a special prismatic layer in front of the solar heat absorber. Under normal conditions, the prismatic layer is transparent but totally reflective above the boiling point of the liquid heating system [21]. Operation temperatures cannot be easily adjusted with this solution as an appropriate fluid (appropriate boiling point) must be selected for each type of solar collector.

Apply an external shading protection for reflecting the incoming solar radiation is a common solution. The manually external shading can be used only for the long periods of no hot water demand. Automated external shading is more practical; it can be activated automatically when the solar fluid reaches a chosen activation temperature. Complexity, cost and dependence on electricity limit the use of this system [8,19].

We studied the thermal behaviour of a flat plate collector equipped with an integrated shading system. The system is a new approach and consists of a reflective protection (aluminium sheet) mounted between the absorber plate and the glass cover. A rotating mechanism for winding and unwinding the aluminium sheet is installed on the top part of the solar collector. This mechanism can be controlled by chosen activation and deactivation temperatures.

As external shading systems, the proposed solution solve the problem at the source, can be adapted to a wide range of solar flat plate collectors and the protection rate of the absorber area can be chosen. Also, the proposed solution protects solar flat plate collectors from overheating without dissipating the heat previously absorbed unlike the case of drain or ventilation systems. Furthermore, the activation and deactivation temperatures can be chosen to satisfy specific technical requirements which depend on the design of the solar flat plate collector. Being inside the solar collector, the proposed integrated shading system is protected against the meteorological hazards. Thus, less expensive and lighter protective materials can be used.

It should be noted that the proposed solution does not work without electric power source and must be designed with high quality standards to avoid access to the interior of the collector in case of failure.

The experimental study was conducted in both laboratory and field conditions. The thermal behaviour of this system has been numerically modelled. Predictions of the numerical model were compared with experimental data for its validation. This report presents some results of this work.

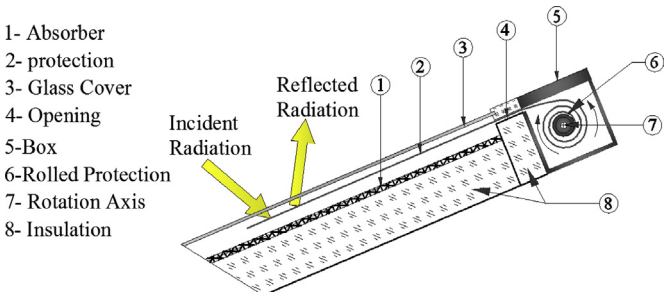

Fig. 1. Schematic of the proposed system.

2. Solution overview

The proposed solution consists of inserting a reflective sheet, in case of overheating, between the absorber plate and the glass cover. The solar radiation is reflected before reaching the absorber plate. The energy transmitted to the circulating fluid is highly reduced and its temperature is significantly lowered. A schematic section of our system can be seen in Fig. 1.

The reflective protection is wrapped around a rotation axis at the top of the solar collector in a special box. The chosen material for the protection is a silver aluminium mirror film. This material has a high reflectivity, low emittance and a good flexibility. In addition, this material is highly resistant to high temperatures. Its reflectance is equal to 0.82 with an absorption coefficient equal to 0.18 and a thermal emittance equal to 0.1.

3. Outdoor tests

3.1. Presentation of the solar facility

The outdoor tests were conducted on solar thermal experimental facility located at University of Miguel Hernandez (UMH), Elche city, Spain on October 2018. The solar facility is installed on the laboratory building roof (see Fig. 2). It includes a solar collector, a pump, an expansion tank and an active heat sink. The solar collector is facing South and its tilt angle measured from the horizontal is equal to 45°. The heat transfer fluid used during the tests is water. The technical characteristics of the tested collector are presented in Table 1.

Fig. 2. Solar testing facility.

Fig. 3. Left: Prototype - Right: Protection mounted on axis.

For the tests, a prototype has been fabricated by modifying a commercial solar collector. The aluminium sheet introduced between the absorber and the glass cover has the following sizes: $850 \times 1900 \times 0.5$ mm. In the upper part of the solar collector frame, an opening was performed in order to introduce the protection. The reflective protection is wrapped around a metallic tube fixed behind the solar collector (see Fig. 3). Two small holes were performed in the lower part of the collector frame in order to allow the crossing of two wires attached to the aluminium sheet. These two wires are used for unwinding, manually, the aluminium sheet.

3.2. Measured data

The ambient temperature and relative humidity, the wind speed and direction and the global solar irradiance in the plane of the solar collector were measured using a meteorological station located very close to the experimental setup (see Fig. 4).

Water temperatures, at the bottom and at the top tubes of the solar collector, are measured using immersed type PT100 in 4-wire connection. The hydraulic circuit pressure was also measured.

The absorber temperature is measured using four K-type thermocouples connected along the rear face of the absorber. The Fig. 5 shows the thermocouples positioning. In this figure, the thermocouples are called T1 to T4. This positioning allows the measurement of the temperature gradient along the absorber's longitudinal

Table 1
Characteristics of the test outside collector.

Glass cover	High resistant solar glass Size: $1000 \times 2040 \times 3.8$ (mm); $\tau_c = 90.8\%$; $\lambda_c = 0.93\ W\ m^{-1}\ K^{-1}$. $C_c = 840\ J\ W^{-1}\ K^{-1}$; $\rho_c = 2500\ kg\ m^{-3}$
Absorber	Copper absorber with a black selective coating. 9 tubes of 8 mm of inner diameter are welded on the back of the absorber. Size: $950 \times 1900 \times 0.8$ (mm); $\alpha_{abs} = 95\%$; $\varepsilon_{abs} = 5\%$ $C_{abs} = 380\ J\ W^{-1}\ K^{-1}$; $\rho_{abs} = 8920\ kg\ m^{-3}$; $\lambda_{abs} = 353.1\ W\ m^{-1}\ K^{-1}$.
Insulation	Back thermal insulation: glass wool, thickness = 50 mm; $\lambda_{ins} = 0.033\ W\ m^{-1}\ K^{-1}$.

Fig. 4. Left: Weather station - Right: Used pyranometer.

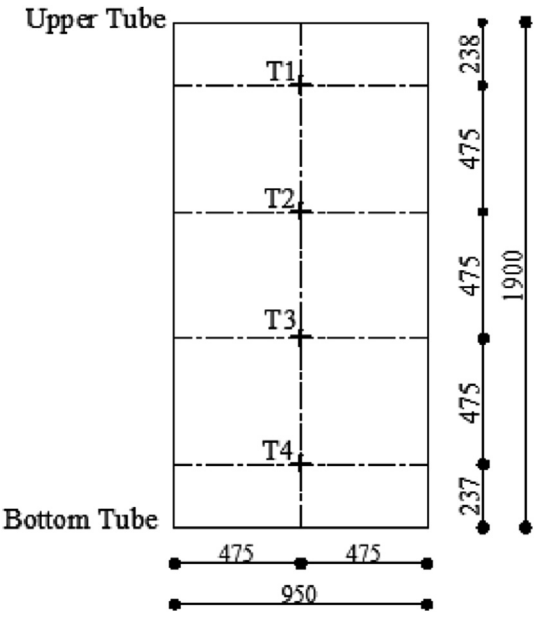

Fig. 5. Thermocouples vertical positions on the absorber surface.

axis in the absorber.

For reading the results, the following symbols are used: $T_{abs,t}$ is the temperature obtained with the T1 thermocouple, $T_{abs,mt}$ is the temperature obtained with the T2 thermocouple, $T_{abs,mb}$ is the temperature obtained with the T3 thermocouple and $T_{abs,b}$ is the temperature obtained with the T4 thermocouple.

The data acquisition system Agilent 34970A was used. The experimental uncertainty was calculated by following [22]. The uncertainties of the measurements have been estimated from the available information from manufacturer's specifications on the possible variability of the measure ("Type B").

Table 2 lists the uncertainties of the measured data for a 95% of confidence level.

3.3. Prototype testing without protection

In this test, the solar collector is not protected and the circulating pump was stopped at 1:00 p.m. The results of the test are shown in Fig. 6 (between 12:30 p.m. and 2:00 p.m.).

During the test time (1.5 h) the solar radiation varied between 1000 and 1050 W/m^2 and the outdoor temperature varied between 25 and 26 °C.

At the beginning of the test, the initial absolute pressure was equal to 3.48 bar and the circulation pump was ON. The water temperature at the top part of the solar collector $T_{w,out}$ was equal to 77.5 °C (outlet) and the water temperature at the bottom $T_{w,in}$ was equal to 71.4 °C (inlet). All absorber temperatures vary between 85 °C and 90 °C. When the pump is turned OFF, $T_{w,out}$ increases to reach the saturation temperature which is equal to 150 °C at equivalent absolute pressure which reach 4.75 bar. Absorber temperatures vary between 150 °C and 197 °C. Measurements indicate that steam is produced. In fact, the temperature at the bottom part of the absorber Tabs,b = 150 °C, which means that it is at saturated conditions. On the contrary, in the medium and top parts, the temperature in the absorber reaches Tabs,t = 197 °C, which means that the steam is overheated.

The steam in the collector is at Tw,out = 150 °C, due to the tube was not insulated and saturated steam was measured where the RTD probe was located.

3.4. Prototype testing with continuous total protection

In this case, the aluminium sheet completely covers the absorber. The pump is stopped all the day (no water circulation). This schedule can occur during a system failure or during long periods of non-use of the solar facility (e.g., holidays). The test results are shown in Fig. 7.

At the beginning of the test and for an incident solar radiation below 350 W/m^2, the water and absorber temperatures at the different positions of the solar collector are close to the ambient temperature (21 °C). Thereafter, at 2:30 p.m., the water temperature at the bottom collector $T_{w,in}$ reaches a maximum of 42 °C and the water temperature at the upper collector $T_{w,out}$ approaches a maximum of 55 °C. This difference of 12 °C is due to the stratification effect in the vertical tubes of the solar collector.

The absorber temperature and the solar radiation curves are highly correlated. When the value of the solar radiation exceeds 1000 W/m^2, the absorber temperature at the top $T_{abs,t}$ reaches a maximum of 74 °C and the absorber temperature at the bottom $T_{abs,b}$ reaches 69 °C. For these temperatures, overheating is avoided. Thus, the absorber coating is protected against excessive temperatures and its physical and optical characteristics are preserved.

Table 2
Uncertainties of the measurements (95% confidence level).

Measured Data	Measurement range	Uncertainty
Outside Air Temperature (RTD Pt100)	−20 - 50 °C	0.3 °C
Relative Humidity of Outdoor Air	0–100%	2%
Wind Direction	0–360°	3°
Wind Speed	0–50 m/s	0.5 m/s
Solar Radiation (Kipp and Zonen CMP 10)	0–1400 W/m^2	23 W/m^2
Water temperature (RTD Pt100)	-50 - 250 °C	0.3 °C
Absorber temperature (Type K Themocouple)	0–250 °C	1.0 °C
Circuit pressure (Omega Pressure Transmitter)	0–6 bar	0.03 bar

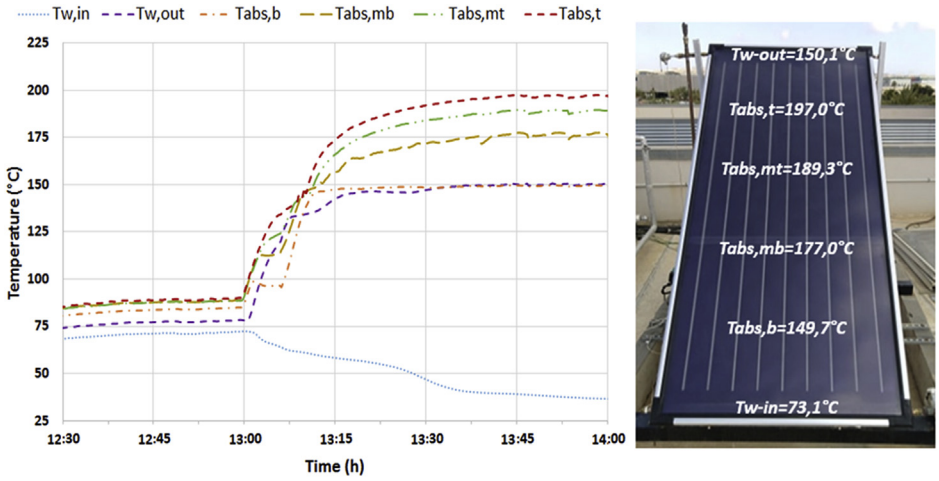

Fig. 6. Collector temperatures variation (case of stagnation) Left: Test results between 1:00 p.m. and 2:00 p.m. - Right: Maximum collector temperatures obtained.

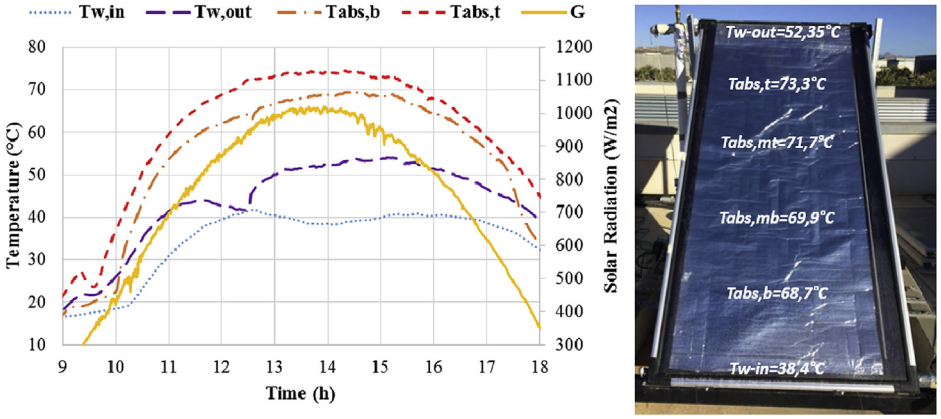

Fig. 7. Temperatures variation of the tested collector with full protection in case of stagnation Left: Test results between 9:00 a.m. and 6:00 p.m. - Right: Test results at 2:00 p.m.

Table 3
Absolute pressures measured.

Percentage of protection	Absolute initial pressure (bar)	Maximum absolute pressure (bar)	Absolute Pressure Difference (bar)	Water temperature at the upper collector (°C)	Equivalent saturation temperature (°C)	Interpretation
75	3.25	3.34	0.09	76.7	138.2	No steam production
50	3.35	3.47	0.12	93.0	138.5	No steam production
25	3.28	3.48	0.20	108.6	138.4	No steam production
0	3.48	4.80	1.32	149.7	149.8	Steam production

Furthermore, there is no risk of steam production in the collector (see Table 3).

3.5. Prototype testing with activation temperature

The test schedule is detailed below (results are shown in Fig. 8). At the beginning of the test, the pump was running and the collector was not protected. The pump stops at 12:33, this leads to a sharp increase in the temperature of the solar collector. When the water temperature in the upper tube of the $T_{w,out}$ collector reaches 120 °C, the protection is activated. The protection remained active for the rest of the test. The activation temperature (120 °C) was chosen to eliminate any risk of the presence of steam since the circuit absolute pressure was 4 bar.

At the beginning of the test, when the pump is running, the water temperature and the temperature of the absorber increase slightly according to the available solar radiation. The water temperature in the upper collector of $T_{w,out}$ is 5 °C higher than the temperature in the lower collector $T_{w,in}$. At 12:33, the bomb is stopped. The temperature of the absorber and the temperature of the water increase rapidly (around 4 °C/min) and at 12:45, $T_{w,out}$ reaches 120 °C and the temperature of the absorber in the upper $T_{abs,\ t}$ reaches 130 °C.

It is observed that after the pump is stopped, the temperature in the bottom tube collector $T_{w,in}$ decreases. This is due to the fact that the water contained in the cold pipes (return circuit) moves

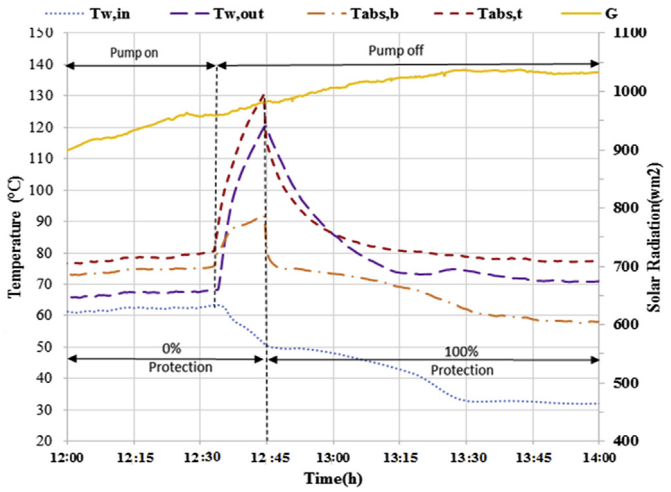

Fig. 8. Temperature measurements of the tested collector protected from an activation temperature equal to 120 °C.

towards the inlet of the solar collector to replace the hot water that rises to the top of the solar collector.

When the temperature at the collector upper tube $T_{w,out}$ reaches 120 °C, the solar collector is fully protected. The absorber temperature at the top $T_{abs,t}$ decreases from 130 °C to 100 °C in less than 12 min (−3 °C/min). This temperature drop continues until thermal stabilization. After 17 min, the absorber temperature at the top $T_{abs,t}$ stabilizes at 79 °C and the absorber temperature at the bottom $T_{abs,b}$ stabilizes at 59 °C. The water temperature at the collector upper tube $T_{w,out}$ stabilizes at 68 °C. Thus, after protection, the overheating is quickly stopped and the risk of steam production is eliminated (see Table 3).

3.6. Prototype testing with partial protection

Tests with partial protection of the solar collector were carried out. Three protection levels, 75%, 50%, 25% were tested. It must be mentioned that in all the cases, the top of the solar collector has been protected, where temperatures are highest without protection (see Fig. 9).

The peak absorber temperature reached for each percentage of protection has been measured between 12:00 and 2:00 p.m. Test results are illustrated in Fig. 9. The tests conditions for each test are listed as follow:

- Collector 75% protected: solar radiation G = 1007 W/m^2; wind speed Ws = 2.4 m/s; ambient temperature T_{amb} = 25 °C;
- Collector 50% protected: solar radiation G = 1010 W/m^2; wind speed Ws = 1.4 m/s; ambient temperature T_{amb} = 26.4 °C;
- Collector 25% protected: solar radiation G = 877 W/m^2; wind speed Ws = 0.7 m/s; ambient temperature T_{amb} = 24.3 °C.

The following observations are:

➢ the absorber temperatures at the bottom $T_{abs,b}$ were measured for the three cases considered in partial protection are very close; they vary between 83 and 86 °C;
➢ the absorber temperatures at the bottom middle $T_{abs,mb}$ for the collectors 50% and 25% protected are almost equal and have the value of 105 °C;
➢ the temperatures of the unprotected parts of the absorber are always higher than the protected parts of the absorber located above; thus, the stratification is not regular;
➢ less we protect the absorber more the absorber temperature at the top middle $T_{abs,mt}$ increases; it can reach 120 °C in the case of a solar collector 25% protected.

These results showed that from 50% of protection, it is possible to avoid easily overheating of the solar system.

3.7. Pressure results

The Table 3 shows the risk of steam production for each case considered. The absolute pressures measured in stagnation condition for 25%, 50% and 75% of protection are close to the initial absolute pressure. Without protection, the absolute pressure in the primary circuit increases by more than 1 bar and steam is produced.

4. Laboratory tests

4.1. Presentation

Laboratory tests were conducted at NanoCorr, Energy & Modelling (NCEM) Research Group, Bournemouth University, United Kingdom. The measurements of the absorber and the glass cover temperatures were performed by using a GUNT ET-202 testing unit [23] (see Fig. 10). The natural sunlight is replaced by a lighting unit with 25 halogen lamps. With this unit, a radiation of

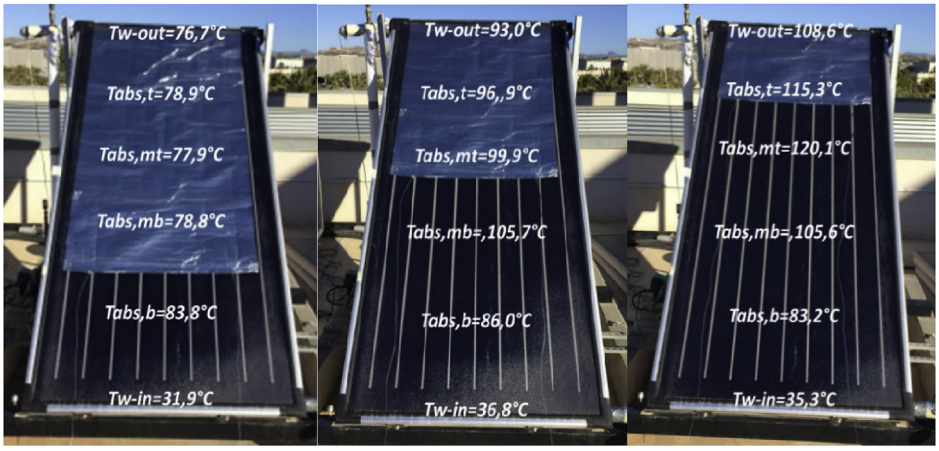

Fig. 9. Left to right tested collector with: 75% of protection - 50% of protection - 25% of protection.

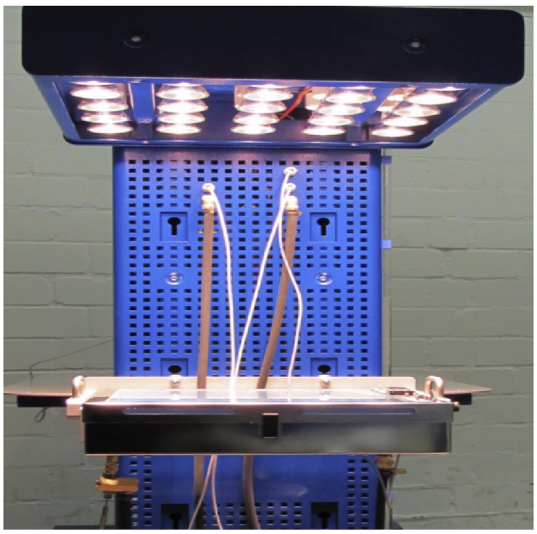

Fig. 10. ET-202 laboratory testing unit [23].

approximately 1152 W/m^2 is obtained. ET-202 unit includes a pump which is switched OFF because the aim in this research was to investigate the stagnation state. ET-202 unit allows for the measurements of various tilt angles of the collector.

During this research, the solar collector is positioned horizontally and the obtained radiation is constant and normal to the solar collector. This highly unfavorable schedule is very different from external conditions. The fluid inside the solar collector was water.

During the tests, the solar collector (450 × 450 mm) was located at a distance of 862 mm from the light source and all the lamps were lit. The laboratory air temperature was stable at 21 °C ± 1 °C. The obtained absorber temperature was the average of three temperatures measured by LM35 temperature sensors [24]. These sensors were positioned in a diagonal pattern. LM35 temperature sensor is an analog sensor which can be operated at temperatures up to 150 °C with a precision between ±0.5 °C and ±1 °C. The glass cover temperature was measured by using a single LM35 temperature sensor located in its center.

The absorber was coated with a non-selective black paint. The protection inserted between the glass cover and the absorber plate is an aluminum foil sheet, the reflective side facing the glass cover and the non-reflective side facing the absorber. The thermal insulation is made with high density polyurethane foam. On the sides, the insulation is 20 mm thick, at the back the insulation is 40 mm thick. The other characteristics of the solar collector used are given in Table 4.

4.2. Experimentation

Three types of tests were conducted in the stagnation case, these are given as follows:

- Test without protection (see Fig. 11); in this case, the solar collector remains unprotected until the stabilization phase of the absorber temperature (about 2 h) was reached.

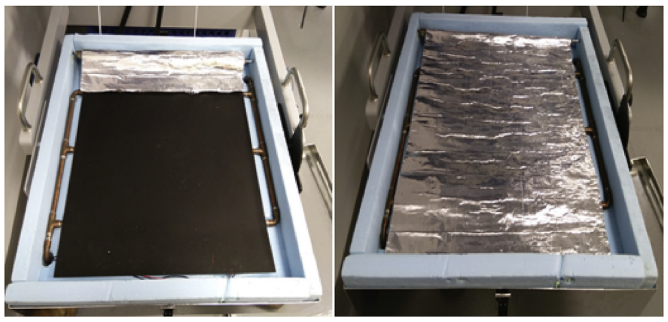

Fig. 11. Left: Collector without protection – Right: Collector with full protection.

- Test with protection (see Fig. 11); in this case, the solar collector remains protected during the test until stabilization (also 2 h) had been achieved.
- Test with activation temperature; at the beginning, the absorber plate is unprotected; when its temperature reaches the activation temperature (called T_{set}), the protection is switched ON until the stabilization phase; three activation temperatures were used as 90, 100 and 110 °C.

At the beginning of the tests, all the components of the solar collector were at the laboratory temperature (21 °C).

The measured values of the absorber temperature for the tested solar collector with protection and without protection are presented in Fig. 12. Without protection, the absorber temperature increases quickly during the first 15 min after the lighting up of the lamps. The absorber temperature reaches 100 °C in about 17 min and converges to a steady-state temperature of 127 °C. In the case of an activated protection, the absorber temperature converges to a steady-state temperature of 73 °C after more than 40 min of a high

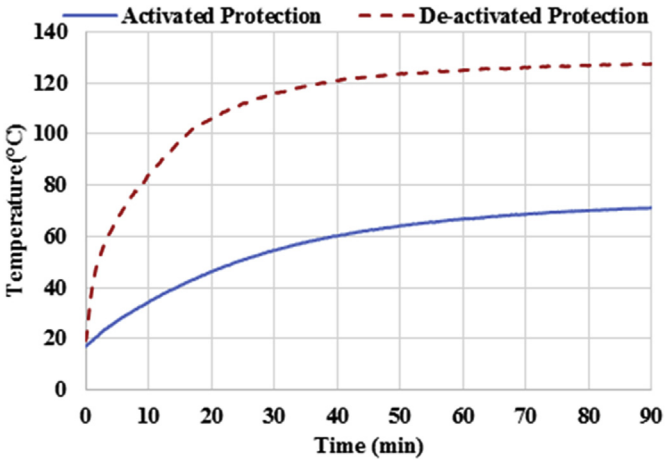

Fig. 12. Absorber temperature variations in stagnation condition of the solar collector tested in laboratory (with and without protection).

Table 4
Characteristics of the solar collector.

Glass cover	Size: 380 × 360 × 3.2 (mm). $\alpha_c = 0.12$; $\varepsilon_c = 0.89$; $\tau_c = 0.85$; $\lambda_c = 0.93\ W\ m^{-1}\ K^{-1}$. $C_c = 840\ J\ W^{-1}\ K^{-1}$ - $\rho_c = 2500\ kg\ m^{-3}$.
Absorber	Size: 340 × 320 × 0.8 (mm). Non selective coating: $\alpha_{abs} = 0.9$ and $\varepsilon_{abs} = 0.9$; $\lambda_{abs} = 353.1\ W\ m^{-1}\ K^{-1}$. $C_{abs} = 380\ J\ W^{-1}\ K^{-1}$; $\rho_{abs} = 8920\ kg\ m^{-3}$.
Protection	Size: 340 × 320 × 0.08 (mm). $C_p = 902\ J\ W^{-1}\ K^{-1}$ and $\rho_p = 2700\ kg\ m^{-3}$; $\lambda p = 237\ W\ m^{-1}\ K^{-1}$.

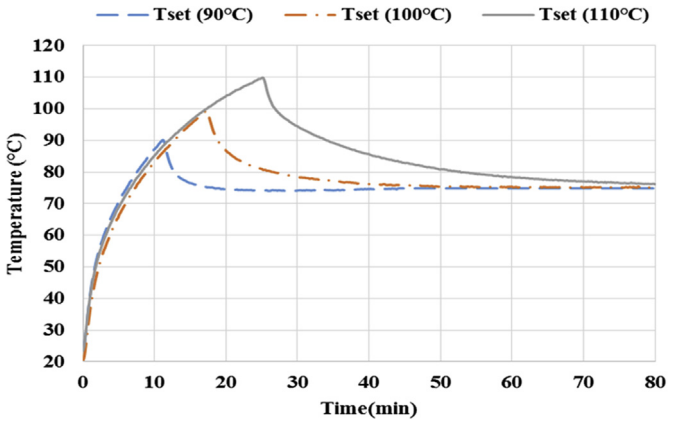

Fig. 13. Laboratory test results of the absorber temperature of the solar collector protected from different activation temperatures in stagnation condition.

radiation (1152 W/m^2), which represents an extreme condition for the solar panel. The difference between the two cases is significant, i.e. 55 °C.

The measured values of the absorber temperature for the tested solar collector for different activation temperatures are presented in Fig. 13. The absorber temperature decreases by more than 15 °C in the first minutes after the activation of the protection for all cases. This rapid decrease allows keeping the absorber out of the overheating zone. The time taken to reach the stabilization phase after activation of the protection is about 15 min for an activation temperature of 90 °C and 45 min for an activation temperature of 110 °C. In all cases, the absorber temperature converges to a steady-state temperature of 78 °C after switching ON the protection. In case of a permanent protection, an almost equal steady-state temperature has been measured (73 °C, see Fig. 12).

5. Modelling and simulations

In practice, the proposed system must be used with a control system. The easiest way is to use the ON/OFF control, solution chosen in this work: the protection is switched ON when the absorber temperature exceeds a temperature called activation temperature and the protection is switched OFF when the absorber decreases below a temperature called deactivation temperature. In order to evaluate the behaviour of the control system, simulations were conducted using a calculation model (see section 5.1). Two cases were tested in this work: solar collector located in Algiers city characterized by a Mediterranean-climate, and solar collector located in Adrar city characterized by a desert climate (see section 5.4).

5.1. Heat transfer equations

In order to model the thermal exchanges within the tested solar collector, we opted for a simplified modelling of the convective and radiative heat transfers. The following assumptions have been adopted:

- The physical characteristics of the glass cover, the absorber, and the insulation are constant.
- The air velocity at the laboratory is constant in the laboratory and is equal to 0.5 m/s.
- In case of laboratory tests, the laboratory walls temperature is equal to the laboratory air temperature.
- The transmittance of the glass cover is constant.

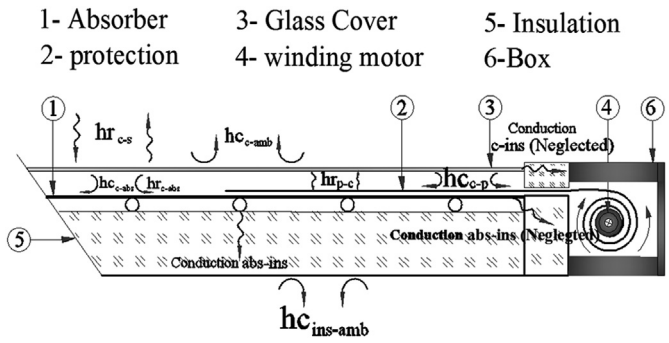

Fig. 14. Heat exchanges representation in flat plat solar collector.

- The physical characteristics of the fluid and of the air gap depend on their temperature.
- The protection is in contact with the absorber once activated.

For the unprotected solar collector, a system of four differential equations is obtained from the energy balance equations applying at the glass cover [25] (equation (1)), at the absorber [25] (equation (2)), at the thermal insulation (equation (3)) and at the heat transfer fluid [26] (equation (4)). The equation system obtained for the simulation of the solar collector without protection is as follows:

$$M_c\, C_c\, dT_c/dt = \alpha_c\, S_c\, G + hr_{c\text{-}s}\, S_c\, (T_s - T_c) + hc_{c\text{-}amb}\, S_c\, (T_{amb} - T_c) + hr_{c\text{-}abs}\, S_c\, (T_{abs} - T_c) + hc_{c\text{-}abs}\, S_c\, (T_{abs} - T_c) \quad (1)$$

$$M_{abs}\, C_{abs}\, dT_{abs}/dt = \tau_c\, \alpha_{abs}\, S_{abs}\, G + hr_{c\text{-}abs}\, S_c\, (T_c - T_{abs}) + hc_{c\text{-}abs}\, S_c\, (T_c - T_{abs}) + \lambda_{tube}/e_{tube}\, S_{abs\text{-}f}\, (T_f - T_{abs}) + \lambda_{ins}/e_{ins}\, S_{abs\text{-}ins}\, (T_{ins} - T_{abs}) \quad (2)$$

$$M_{ins}\, C_{ins}\, dT_{ins}/dt = \lambda_{ins}/e_{ins}\, S_{abs\text{-}ins}\, (T_{abs} - T_{ins}) + hc_{ins\text{-}amb}\, S_{ins}\, (T_{amb} - T_{ins}) \quad (3)$$

$$M_f\, C_f\, dT_f/dt = \lambda_{tube}/e_{tube}\, S_{abs\text{-}f}\, (T_{abs} - T_f) \quad (4)$$

For the protected solar collector presented in Fig. 14, a system of five differential equations is obtained from the energy balance equations applying at the glass cover (equation (5)), at the protection (equation (6)) and at the absorber (equation (7)). Equations (3) and (4) seen previously remain unchanged. We obtain the following system of equations:

$$M_c\, C_c\, dT_c/dt = \alpha_c\, S_c\, G + \alpha_c\, \tau_c\, S_c\, G\, (1 - \alpha_p) + hr_{c\text{-}s}\, S_c\, (T_s - T_c) + hc_{c\text{-}amb}\, S_c\, (T_{amb} - T_c) + hr_{c\text{-}p} S_c\, (T_p - T_c) + hc_{c\text{-}p} S_c\, (T_p - T_c) \quad (5)$$

$$M_p\, C_p\, dT_p/dt = \tau_c\, \alpha_p\, S_p\, G + hr_{c\text{-}p}\, S_c\, (T_c - T_p) + hc_{c\text{-}p}\, S_c\, (T_c - T_p) + \lambda_P/e_P\, S_{abs\text{-}P}\, (T_{abs} - T_P) \quad (6)$$

$$M_{abs}\, C_{abs}\, dT_{abs}/dt = \lambda_P/e_P\, S_{abs\text{-}P}\, (T_P - T_{abs}) + \lambda_{tube}/e_{tube}\, S_{abs\text{-}f}\, (T_f - T_{abs}) + \lambda_{ins}/e_{ins}\, S_{abs\text{-}ins}\, (T_{ins} - T_{abs}) \quad (7)$$

During the laboratory experiments, we have radiative heat transfer between the glass cover and the walls of the laboratory. In the equation (1), the sky temperature is replaced by the laboratory temperature (21 °C). The convective heat transfer coefficient between the room air and the walls is assumed to be constant and equals to 4.5 W/m^2.K. The calculation formulae concerning the other convection heat transfer coefficients are given in the appendix.

The calculations were performed by using numerical models built in the MATLAB/Simulink graphical environment. To solve the

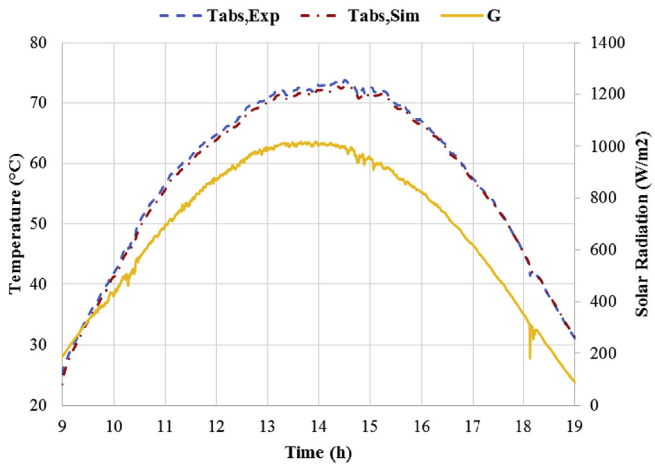

Fig. 15. Absorber temperature results of outdoor test and numerical simulation in stagnation condition (collector fully protected).

systems of equations, various methods were used such as Runge Kutta of order 4 and Euler's method.

5.2. Validation with outdoor tests

For the validation of the numerical model, we compared the measured and calculated values of the absorber temperature (see Fig. 15). The experimental results developed with total and permanent protection were used. The mean absolute percentage error between experimental and numerical data is 1.26%.

5.3. Validation with laboratory tests

For the validation with laboratory tests, we compared the experimental results for two cases: with protection and without protection (see Fig. 16). The temperatures measured and calculated are similar, very close and converge to the same steady-state temperatures. The mean absolute percentage error between experimental and numerical results varies between 2.76% and 6.20%.

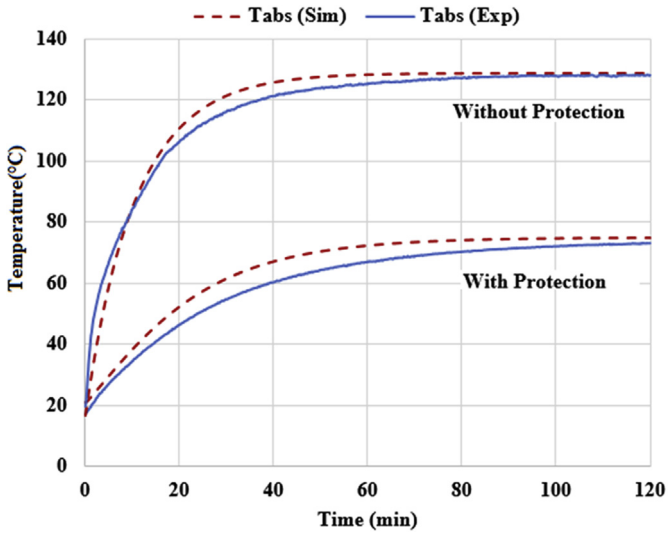

Fig. 16. Absorber temperature results of laboratory test and numerical simulation in stagnation condition (with and without protection).

Simulation results in both cases (with and without protection) are higher than experimental results, especially from the 20th to the 60th minute. From the 80th minute, simulation and experimental results tend to stabilize to the same value: 127 °C without protection and 74 °C with protection.

Based on these results, the simplified numerical model can be considered acceptable. In our opinion, it's not necessary to use more complex modelling techniques at this stage of the study.

5.4. Application of the numerical model

Numerical simulations in were first performed for a solar collector located in Algiers city: latitude equal to 36.7° N, longitude equals to 3.06° E. Solar collector used for the simulations has similar characteristics to solar collectors seen during the tests. The solar collector is facing south and its tilt angle measured from the horizontal is equal to 45° and the circulating pump is off. The simulations were performed on July 21st. The city of Algiers is characterized by a Mediterranean-climate. The outside temperature varies between 25 °C at five o'clock in the morning and 34 °C at three o'clock in the afternoon. Fig. 17 shows climatic data adopted for the simulations.

The protection system works in the following way. The protection is switched on as soon as the absorber temperature exceeds 90 °C. It is switched off as soon as the absorber temperature decreases below 70 °C. The results of the simulations are shown in Fig. 18.

At about 10:00 h in the morning, the absorber temperature reaches the activation temperature of 90 °C. At this time, the protection is switched ON and the absorber temperature decreases and reaches the activation temperature of 70 °C after 15 min. At this time, the protection is switched OFF and the absorber temperature increases and reaches the deactivation temperature of 90 °C after 13 min. This cycle is repeated twelve times a day.

In the second step, the simulations were performed for the same solar collector located in Adrar city: latitude equals to 27.97 °N, longitude equals to 0.187° W. The circulating pump is off. The Adrar city is characterized by a desert climate. Fig. 19 shows climatic data adopted.

Until 05:30 p.m. and after the second operating cycle, the protection remains switched ON and the absorber temperature remains above 70 °C (see Fig. 20). The cycling behaviour disappears because even protected the absorber temperature doesn't decrease to reach the deactivation temperature of protection, this is due to the high value of the outside temperature. The protection is switched OFF at 05:30 p.m. after the decrease of the solar radiation.

For the two cases, time between starts of the rotating systems does not exceed 15 min, which seems acceptable.

6. Conclusion

In this work, a new solution to prevent high temperatures and steam production due to stagnation in the solar collectors has been successfully tested. The proposed solution consists of inserting a sheet of aluminium, in case of stagnation, between the absorber plate and the glass cover. This protection may be total or partial. A prototype has been manufactured and tested.

The experimental study was conducted in both laboratory and outdoor conditions. Tests with an activation temperature were led: at the beginning, the absorber plate is unprotected; when its temperature reaches an activation temperature, the protection is switched ON until the stabilization. Several coverage rates have been tested in field conditions.

A numerical model of the thermal behaviour of the solar collector was developed and validated with experimental results. This

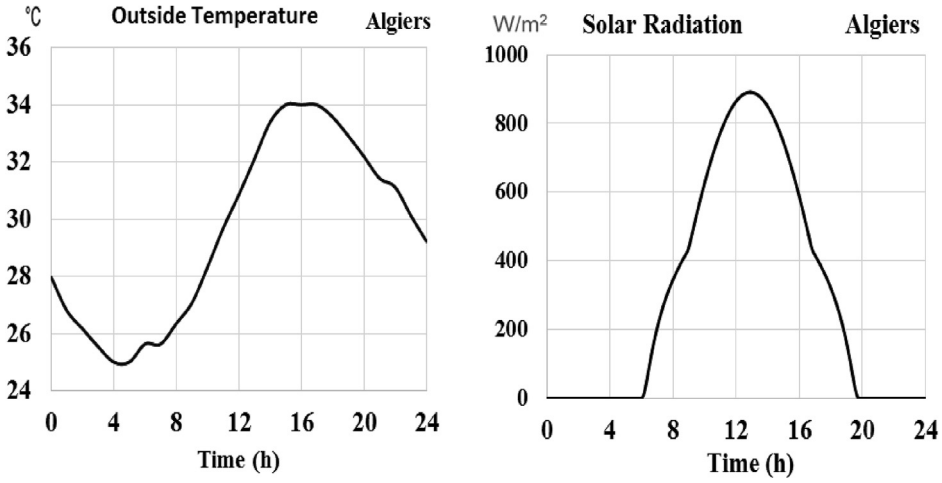

Fig. 17. Climatic data – Algiers city.

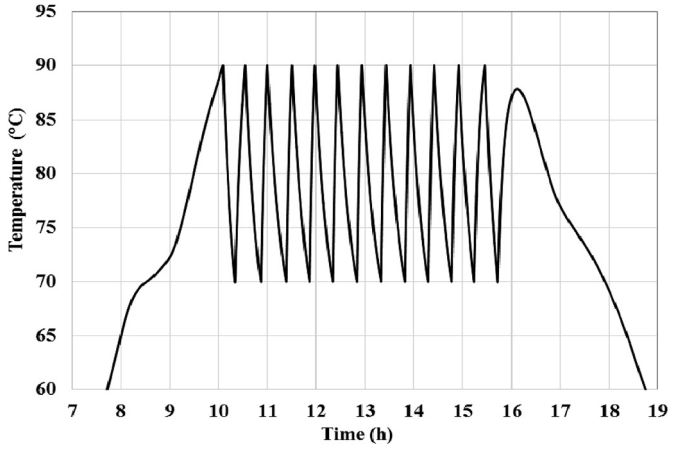

Fig. 18. Simulation results of absorber temperature – Collector located in Algiers city.

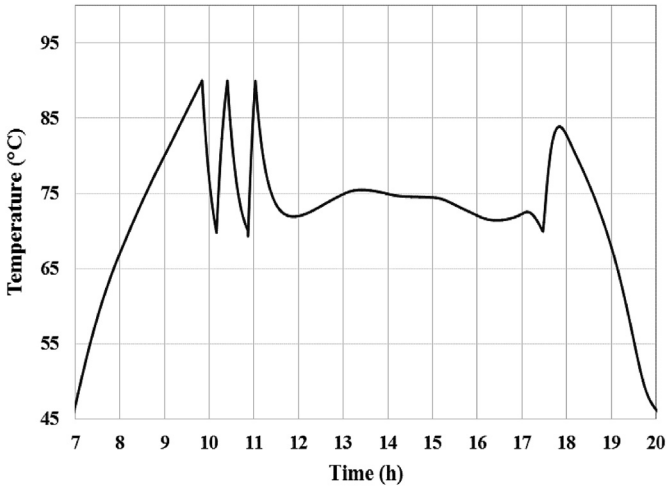

Fig. 20. Simulation results of absorber temperature – Collector located in Adrar city.

model takes into account only the cases of solar collectors without protection or with full protection.

The experimental tests and calculations show that the solution gives good results. Based on outdoor tests, we show that from 50% of partial protection, it is possible to avoid easily overheating. Based on laboratory tests, when the solar collector subjected to extreme solar radiation (normal radiation of 1152 W/m^2) is fully protected, the absorber temperature does not exceed 80 °C. In addition, the proposed system can be adapted to a wide range of solar thermal panels.

Based on the results obtained, the proposed solution can be considered as promising to prevent overheating of solar collectors.

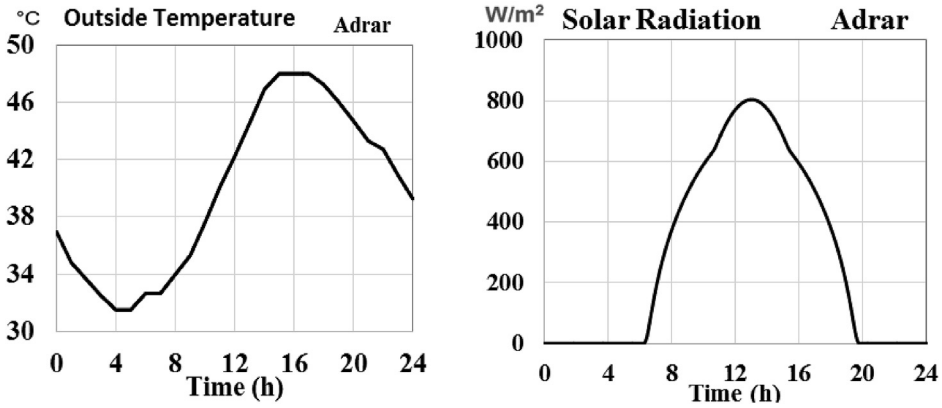

Fig. 19. Climatic data –Adrar city.

During the tests, the overheating protection system has been moved manually. We have developed a preliminary design of thermal solar collector with a motorized rotary mechanism which allows an automated movement of the protection by using the electrical power. Future works will aim to make the proposed system less dependent on the electrical grid. This device could be powered by rechargeable batteries or by photovoltaic cells.

Many factors influencing the switch-on frequency of the control system are the tilt angle, orientation, size and efficiency of the solar collector, activation temperature values and weather conditions. Future works will study the influence of these parameters.

It is also remains to build a numerical model which takes into account the heat transfers in the partial protection case. Future works will take over this aspect.

Author contributions

A.AMICHE: Conceived and designed the analysis, Collected the data, Contributed data or analysis tools, Performed the analysis, Wrote the paper, Other contribution. S. M. K. EL HASSAR: Collected the data, Collected the data, Contributed data or analysis tools, Performed the analysis, Wrote the paper, Other contribution. A. LARABI: Contributed data or analysis tools, Other contribution. Z.A. KHAN: Contributed data or analysis tools, Wrote the paper, Other contribution. Z. KHAN: Contributed data or analysis tools, Contributed data or analysis tools, Wrote the paper, Other contribution. F. J. AGUILAR: Collected the data, Contributed data or analysis tools, Performed the analysis, Wrote the paper, Other contribution. P. V. QUILES: Collected the data, Contributed data or analysis tools, Performed the analysis, Wrote the paper, Other contribution.

Acknowledgments

The authors would like to thank the NCEM Research Group, Bournemouth University, United Kingdom, and the Department of Mechanic Engineering and Energy, University of Miguel Hernández, DMEE, UMH, Spain, for supporting experimental work, significant contributions in making this research possible and hosting the University of Sciences & Technology Houari Boumediene (USTHB) visiting researcher.

Appendix. Heat transfer coefficients

Heat exchange between	Formula
Glass cover and Absorber	$hc = \frac{Nu \times e}{\lambda}$ With $Nu = 1 + 1,44\left[1 - \frac{1708(\sin 1,8\ \beta)^{1.6}}{Ra\cos\beta}\right]\left[1 - \frac{1708}{Ra\cos\beta}\right] + \left[\left(\frac{Ra\cos\beta}{5830}\right)^{\frac{1}{3}} - 1\right]$
Glass cover and Protection	$hc = \frac{Nu \times (e/2)}{\lambda}$ with$Nu = 1 + 1,446(1 - 1708/Ra\cos\beta)$

e: distance in meters between two faces.
λ: Conductivity in W m^{-1} K^{-1} of the air (air gap).
β: Tilt angle in degrees of the solar collector.
Nu: Nusselt Number.

Ra: Rayleigh Number for the air (air gap). The heat transfer due radiation (hr) between two surfaces is estimated by considering them as two infinitely parallel grey surfaces. This hypothesis allows the use of the equation cited below to calculate the radiative heat transfer coefficient between two surfaces 1 and 2. If the temperatures of the two surfaces are T_1 and T_2 and if the emittance of the two surfaces are ε_1 and ε_2, we have:

$$hr = \frac{\sigma(T_1 + T_2)\left(T_1^2 + T_2^2\right)}{\frac{1}{\varepsilon_1} + \frac{1}{\varepsilon_2} - 1}$$

References

[1] R. Sellami, et al., Market potential and development prospects of the solar water heater field in Algeria, Renew. Sustain. Energy Rev. 65 (2016) 617–625 (Elsevier Editions).
[2] S.M.K. El Hassar, "*Guide pour une construction éco-énergétique en Algérie*", livre, Editions Universitaires Européennes, Allemagne, 2016.
[3] L. Zhou, et al., Q. "*CFD investigation of a new flat plate collector with additional front side transparent insulation for use in cold regions*, Renew. Energy 138 (2019) 754–763. Elsevier Editions.
[4] M.E. Zayed, et al., Performance Augmentation of Flat Plate Solar Water Collector Using Phase Change Materials and Nanocomposite Phase Change Materials: A Review, Process Safety and Environmental Protection, 2019.
[5] T. Beikircher, et al., Advanced solar flat plate collectors with full area absorber, front side film and rear side vacuum super insulation, Sol. Energy Mater. Sol. Cells 141 (2015) 398–406.
[6] G. Colangelo, et al., Innovation in flat solar thermal collectors: a review of the last ten years experimental results, Renew. Sustain. Energy Rev. 57 (2016) 1141–1159.
[7] P.V. Quiles, F.J. Aguilar, S. Aledo, Analysis of the overheating and stagnation problems of solar thermal installations, Energy Procedia J. 48 (2014) 172–180.
[8] S. Harrison, et al., A review of strategies for the control of high-temperature stagnation in solar collectors and systems, Energy Procedia J. 30 (2012) 793–804 (Elsevier Editions).
[9] Overheating protection for solar collectors", ww.radiantcompany.com/system/solar/heatdump/. Accessed April 2017.
[10] E. Frank, et al., Overheating Prevention and Stagnation Handling in Solar Process Heat Applications, International Energy Agency-Solar Heating and Cooling, 2015. IEA SHC Task49.
[11] R. Botpaev, et al., Drain-back solar thermal systems: a review, Sol. Energy 128 (2016) 41–60.
[12] A. Martínez, et al., Thermoelectric self-cooling system to protect solar collectors from overheating, J. Electron. Mater. 43 (2014) 1480–1486.
[13] H. Kessentini, et al., Development of a plate collector with plastic transparent insulation and low-cost overheating protection system, Appl. Energy J. 133 (2014) 206–223. Elsevier Editions.
[14] D. Kizildag, et al., Development, optimization and test performance of highly efficient flat plate solar collector with transparent insulation and low-cost overheating protection, in: ISES Solar World Congress 2017, in Proceedings IEA SHC International Conference on Solar Heating and Cooling for Buildings and Industry, International Solar Energy Society, 2017, pp. 2031–2042.
[15] H. Shafqat, S.J. Harrison, Experimental and numerical investigations of passive air-cooling of a residential flat-plate solar collector under stagnation conditions, Sol. Energy 122 (2015) 1023–1036.
[16] S. Föste, et al., Flat plate collectors with thermochromic absorber coatings to reduce loads during stagnation, Energy Procedia J. 91 (2016) 42–48 (Elsevier Editions).
[17] D. Mercs, et al., Innovative smart selective coating to avoid overheating in highly efficient thermal solar collectors, Energy Procedia J. 91 (2016) 84–93 (Elsevier Editions).
[18] A. Paone, et al., Thermal solar collector with VO2 absorber coating and V1-xWxO2 thermochromic glass cover Temperature matching and triggering, Solar Energy J. 110 (2014) 151–159 (Elsevier Editions).
[19] A. Amiche, et al., Flat plate collectors with thermochromic absorber coatings in the Algerian context, in: Proceedings Book of 1st International Conference on Energy and Thermal Engineering, April 25-28, Istanbul, Turkey, 2017, pp. 387–391.
[20] M. Neagoe, et al., A new approach on the protection against overheating of flat plate solar-thermal collectors, in: Conference on Sustainable Energy, Springer, Cham, 2017, pp. 283–295.
[21] M. Slaman, R. Griessen, Solar collector overheating protection, Sol. Energy 83 (2009) 982–987.
[22] JCGM 100:2008, Evaluation of Measurement Data – Guide to the Expression of Uncertainty in Measurement.
[23] K. Boedecker, Experiment Instructions ET 202 – Principles of Solar Thermal Energy, Manuel, GUNT Gerätebau, Barsbüttel, Germany, august 2011.
[24] National SemiConductor, NSC (Texas Instruments), LM35 Precision Centigrade Temperature Collectors, Technical Document, 2016.
[25] M. Hamed, et al., Parametric sensitivity studies on the performance of a flat plate solar collector in transient behavior, Energy Conv. Manag. J. 78 (2014) 938–947 (Elsevier Editions).
[26] J. Watmuff, et al., Solar and wind induced external coefficients for solar collectors, Rev. Int. D. Hepatol. 2 (1977) 56.